

See discussions, stats, and author profiles for this publication at: <https://www.researchgate.net/publication/257826909>

# Revised Coefficients for Priestley–Taylor and Makkink–Hansen Equations for Estimating Daily Reference Evapotranspiration

Article in *Journal of Hydrologic Engineering* · October 2013

DOI: 10.1061/(ASCE)HE.1943-5584.0000679

CITATIONS

46

READS

1,401

4 authors, including:



**Nicoleta C. Cristea**

University of Washington Seattle

27 PUBLICATIONS 507 CITATIONS

[SEE PROFILE](#)



**Stephanie Kampf**

Colorado State University

59 PUBLICATIONS 1,297 CITATIONS

[SEE PROFILE](#)



**Stephen J. Burges**

University of Washington Seattle

152 PUBLICATIONS 8,054 CITATIONS

[SEE PROFILE](#)

Some of the authors of this publication are also working on these related projects:



Hydrology, geomorphology, and ecology of intermittent rivers and ephemeral streams [View project](#)



Develop an Integrated System to Maximize the Return of Investing in Fire Resilient Watersheds in the Interior West [View project](#)

# Revised Coefficients for Priestley-Taylor and Makkink-Hansen Equations for Estimating Daily Reference Evapotranspiration

Nicoleta C. Cristea<sup>1</sup>; Stephanie K. Kampf<sup>2</sup>; and Stephen J. Burges, F.ASCE<sup>3</sup>

**Abstract:** Many applications require estimation of reference evapotranspiration ( $ET_o$ ) in areas where meteorological measurements are limited. Previous studies have shown that simple evapotranspiration models based on radiation and temperature perform relatively well in humid climates but underpredict  $ET_o$  in drier and windier climates. In this paper, estimates of  $ET_o$  based on existing simple models were compared with  $ET_o$  calculated with the more comprehensive Penman-Monteith equation using meteorological measurements at 106 locations in the contiguous United States for a range of climates. Results showed that the simpler models were closest to the more comprehensive model at sites where the annual mean relative humidity (RH) was approximately 70% and annual 2-m wind speed ( $U$ ) was less than  $2 \text{ m} \cdot \text{s}^{-1}$ . Equations for adjusting the model coefficients were developed based on annual averages of RH [or vapor pressure deficit (VPD)] and  $U$  to improve the performance of these models for drier and windier sites. Publicly available data sets of spatial distributions of annual RH and  $U$  were used to estimate local coefficients for the contiguous United States. The new coefficients were tested with additional data from 22 sites, not used for coefficient development. At the test sites, the performance of both tested models improved with the revised coefficients. Depending on the model, 63–90% of the stations had  $ET_o$  within 10% of the Penman-Monteith  $ET_o$  for the growing season. The revised coefficients can be used to improve estimation of reference  $ET_o$  in data-limited applications such as remote sensing and distributed hydrologic modeling. DOI: 10.1061/(ASCE)HE.1943-5584.0000679. © 2013 American Society of Civil Engineers.

**CE Database subject headings:** Evapotranspiration; Coefficients; Hydrologic models; Measurement.

**Author keywords:** Reference evapotranspiration; Priestley-Taylor model; Makkink model; Evaporative coefficients; Evapotranspiration models.

## Introduction and Background

Radiation-based evapotranspiration models such as Priestley and Taylor (PT) (1972) are widely used in hydrologic modeling [e.g., Bandaragoda et al. (2004), Wang et al. (2006b), Schramm et al. (2007), and Soyulu et al. (2011)] and many other ecological applications. The PT model was derived for saturated conditions and open water sites where wind effects were negligible. The wind function multiplied by the vapor pressure deficit term in the Penman (1948) equation was eliminated, and the evaporative coefficient  $\alpha$  was introduced, with an estimated average value of 1.26. This coefficient was later found to vary, depending on land cover and site conditions, and a relatively wide range of  $\alpha$  (0.6–2.47) has been reported (Table 1). High values of  $\alpha$  were found at dry and windy sites, and low values of  $\alpha$  were found at humid sites, mostly in Canada, but also in other parts of the world

[e.g., Kustas et al. (1996) and Eaton et al. (2001)]. Compared with lysimeter data, the Priestley-Taylor model with  $\alpha = 1.26$  was found to underpredict significantly in windy and arid conditions (Berengena and Gavilán 2005; Benli et al. 2010), and to overpredict slightly in humid conditions (Yoder et al. 2005).

Another radiation-based model for calculating evapotranspiration, Makkink (1957), was also derived from Penman's model and was validated with lysimeter measurements collected in the Netherlands for short grass. De Bruin (1981, 1987) proposed modifications of the original Makkink model. Based on further research in the Netherlands and Denmark, the Makkink evaporative coefficient  $C$  was established equal to 0.7 (Hansen 1984). The Makkink method with the Hansen correction, referred to as the Makkink-Hansen (MK-Ha) method, compared well with lysimeter data at a humid location in Germany (Xu and Chen 2005). Descriptions of both Priestley-Taylor and Makkink-Hansen models are given in "Daily Evapotranspiration Models."

A more comprehensive physically based model used to compute evapotranspiration is the Penman-Monteith model. The Food and Agriculture Organization of the United Nations (FAO) Irrigation and Drainage Paper 56 version of the Penman-Monteith model (FAO-56 PM) established the computational steps needed to calculate reference evapotranspiration  $ET_o$  from a well-watered surface of green grass of specified height, albedo, and surface resistance (Allen et al. 1998). The FAO-56 PM model has been shown consistently to perform well against measured data in a variety of climates (Garcia et al. 2004; Yoder et al. 2005; López-Urrea et al. 2006; Gavilán et al. 2007; Benli et al. 2010). Compared with the radiation-based models, PT and MK-Ha, that use as inputs net radiation ( $R_n$ ) or solar radiation ( $R_s$ ) and temperature ( $T$ ), the

<sup>1</sup>159 Wilcox Hall, Box 352700, Univ. of Washington, Seattle, WA 98195-2700 (corresponding author). E-mail: cristn@u.washington.edu

<sup>2</sup>B248 Natural and Environmental Sciences Building, Colorado State Univ., Fort Collins, CO 80523-1476. E-mail: Stephanie.Kampf@colostate.edu

<sup>3</sup>160 Wilcox Hall, Box 352700, Univ. of Washington, Seattle, WA 98195-2700. E-mail: sburges@u.washington.edu

Note. This manuscript was submitted on August 24, 2011; approved on June 27, 2012; published online on August 4, 2012. Discussion period open until March 1, 2014; separate discussions must be submitted for individual papers. This paper is part of the *Journal of Hydrologic Engineering*, Vol. 18, No. 10, October 1, 2013. © ASCE, ISSN 1084-0699/2013/10-1289-1300/\$25.00.

**Table 1.** Estimated Values of the PT Evaporative Coefficient  $\alpha$  for a Range of Climates and Terrain Covers

Reference	$\alpha$	Local conditions and study site
Pereira (2004)	1.26	Perennial ryegrass, semiarid, Davis, CA
	1.27	Grass, humid tropical, Piracicaba, SP, Brazil
Zhang et al. (2004)	1.17, 1.26	Winter wheat, semiarid monsoon climate. North China Plain
	1.06, 1.09	Maize, semiarid monsoon climate North China Plain
Castellvi et al. (2001)	1.2–1.9	Reference grass, semiarid, northeast Spain, monthly $\alpha$
Kustas et al. (1996)	0.6–1.0	Mixture of rangeland, pasture and cropland, continental climate, Chickasha, OK, half-hourly time step
Flint and Childs (1991)	0.9	Partially vegetated clear cut forest site in southwest Oregon, water limited, $\alpha$ was related to soil moisture
Fisher et al. (2005)	0.73, 0.94	Ponderosa pine forest ecosystem at an AmeriFlux site in northern California
Daneshkar Arasteh and Tajrishy (2008)	1.20–2.47	Open water, arid conditions, Chahnimeh Reservoir, southeast Iran
Gavin and Agnew (2004)	0.8–1.25	Wet grassland, southeast England
Eaton et al. (2001)	1.51–2.32	Deep lake (Great Slave Lake), Northwest Territories, Canada
	1.17–1.45	Shallow lake (Golf Lake), Churchill, Manitoba, Canada
	1.07–1.10	Wetland tundra, Trail Valley Creek basin, Northwest Territories, Canada
	0.83–1.46	Sedge wetland, Churchill, Manitoba, Canada
	1.00–1.08	Shrub tundra, Trail Valley Creek basin, Northwest Territories, Canada
	0.95–1.20	Shrub tundra, Churchill, Manitoba, Canada
	0.81–1.00	Upland tundra, Churchill, Manitoba, Canada
	0.77	Forest, Havikpak Creek, Northwest Territories, Canada
	0.94–0.95	Churchill spruce–tamarack forest Manitoba, Canada
Souch et al. (1996)	1.035	Wetlands in the Indiana Dunes National Lakeshore near Lake Michigan, Indiana, hourly time step
Stewart and Rouse (1976) <sup>a</sup>	1.26	Shallow lake, Hudson Bay Coast, Ontario, Canada
Bello and Smith (1990) <sup>a</sup>	1.35	Shallow lake, Northern Manitoba, Canada
Rouse et al. (1977) <sup>a</sup>	1.26	Wetland, Hudson Bay Coast, Ontario, Canada
Price et al. (1991) <sup>a</sup>	1.20	Wetland, Lake Melville, Newfoundland, Canada
Rouse et al. (1977) <sup>a</sup>	0.95	Upland tundra, Hudson Bay Coast, Ontario, Canada
	1.13	Coniferous forest, Lake Athabasca, Northwest Territories, Canada
Jury and Tanner (1975) <sup>b</sup>	1.57	Strongly advective conditions
Mukammal and Neumann (1977) <sup>b</sup>	1.29	Grass, soil at field capacity
Davies and Allen (1973) <sup>b</sup>	1.27	Irrigated ryegrass
McNaughton and Black (1973) <sup>b</sup>	1.18	Wet Douglas fir forest
	1.05	Douglas fir forest
De Bruin and Holtslag (1982) <sup>b</sup>	1.12	Short grass
Barton (1979) <sup>b</sup>	1.04	Bare soil surface
Black (1979) <sup>b</sup>	0.84	Douglas fir unthinned
	0.8	Douglas fir thinned
Giles et al. (1985) <sup>b</sup>	0.73	Douglas fir forest (daytime)
Shuttleworth and Calder (1979) <sup>b</sup>	0.72	Spruce forest (daytime)

<sup>a</sup>Cited in Eaton et al. (2001).<sup>b</sup>Originally cited in Flints and Childs (1991) and relisted in Fisher et al. (2005).

FAO-56 PM model is more data intensive, requiring in addition to  $R_s$  and  $T$  relative humidity (RH) and wind speed at 2-m height ( $U$ ). Even though the PT and MK-Ha models have shown varying effectiveness in prior studies, the parsimonious structure and limited data requirements make these models attractive alternatives to the Penman-Monteith model in applications with limited data or in remote sensing applications [e.g., Jiang and Islam (2001), Wang et al. (2006a), and Bois et al. (2008)].

To improve the PT and MK-Ha performance, relationships have been developed to adjust the PT and MK-Ha evaporative coefficients using mean annual values of RH [or vapor pressure deficit (VPD)] and  $U$ . The coefficients are estimated for grass but can be modified for other land cover types through crop factors. Because of the limited availability of observed  $ET_o$  data sets, the FAO-56 PM  $ET_o$  estimates have been used as surrogates for measured data. Due to its broad acceptance, the FAO-56 PM is now routinely used as a base for comparison for simpler  $ET_o$  calculation methods (Irmak et al. 2003a), to adjust or calibrate other  $ET_o$  methods (Tabari and Hosseinzadeh Talaei 2011), or to develop new methods [e.g., Irmak et al. (2003b)]. The coefficients developed in this paper can be estimated from publicly available geographic

information system (GIS) data sets and can provide reliable  $ET_o$  estimates in situations with limited meteorological data.

The objectives of this paper are to (1) characterize the annual RH and  $U$  conditions for which the PT and MK-Ha  $ET_o$  predictions differ from FAO-56 PM  $ET_o$  and quantify the magnitude of these discrepancies, (2) develop and test coefficient adjustment relationships for the PT and MK-Ha models based on annual average RH (or VPD) and  $U$ , and provide maps of the adjusted coefficients, and (3) show which of the two methods performs best in comparison with FAO-56 PM at a daily time scale when using the original and newly developed coefficients. All findings are for the daily time step PT and MK-Ha models with applicability for the contiguous United States.

## Daily Evapotranspiration Models

### FAO 56 Penman-Monteith Model

The daily time step FAO-56 PM model [Eq. (1)] estimates  $ET_o$  for the reference surface, defined as the hypothetical reference crop

with an assumed crop height of 0.12 m, a fixed surface resistance of  $70 \text{ s m}^{-1}$  and an albedo of 0.23, resembling “an extensive surface of green, well-watered grass of uniform height actively growing and shading the ground” (Allen et al. 1998):

$$ET_o = \frac{0.408\Delta(R_n) + \gamma \frac{900}{T+273} U(e_s - e_a)}{\Delta + \gamma(1 + 0.34U)} \quad (1)$$

where  $ET_o$  = FAO-56 PM reference evapotranspiration ( $\text{mm day}^{-1}$ );  $R_n$  = calculated mean daily net radiation at the grass surface ( $\text{MJ m}^{-2} \text{ day}^{-1}$ );  $T$  = mean daily air temperature at 2-m height ( $^{\circ}\text{C}$ );  $U$  = mean daily wind speed at 2-m height ( $\text{m s}^{-1}$ );  $e_s$  = saturation vapor pressure (kPa), calculated as the average of saturation vapor pressures at the maximum and the minimum air temperatures;  $e_a$  = daily mean actual 2-m height vapor pressure (kPa);  $\Delta$  = slope of the saturation vapor pressure-temperature curve ( $\text{kPa}^{\circ}\text{C}^{-1}$ ); and  $\gamma$  = psychrometric constant ( $\text{kPa}^{\circ}\text{C}^{-1}$ ). Details for calculating the daily values of  $\Delta$ ,  $\gamma$ ,  $R_n$ ,  $e_s$ , and  $e_a$  are provided in Allen et al. (1998). The VPD was estimated as  $e_s - e_a$  (kPa).

### Priestley-Taylor Model

The equation used to compute daily  $ET_o$  rates with the PT model is

$$ET_{oPT} = \alpha \frac{\Delta}{\Delta + \gamma} \frac{R_n}{\lambda} \quad (2)$$

where  $ET_{oPT}$  = PT reference evapotranspiration ( $\text{mm day}^{-1}$ );  $\alpha = 1.26$ , the PT evaporative coefficient (-); and  $\lambda$  = latent heat of vaporization at  $20^{\circ}\text{C}$  ( $2.45 \text{ MJ kg}^{-1}$ ). Values of  $\Delta$ ,  $\gamma$ , and  $R_n$  are calculated using the same procedure as for the FAO-56 PM model.

### Makkink-Hansen Model

The Makkink method was used with the Hansen (1984) correction to compute daily  $ET_o$  rates as

$$ET_{oMK-Ha} = C \frac{\Delta}{\Delta + \gamma} \frac{R_s}{\lambda}, \quad (3)$$

where  $ET_{oMK-Ha}$  = reference evapotranspiration ( $\text{mm day}^{-1}$ );  $C = 0.7$ , the evaporative coefficient proposed by Hansen (1984);  $R_s$  = mean daily solar radiation ( $\text{MJ m}^{-2} \text{ day}^{-1}$ ); and the remaining variables are defined using the same procedure as in the FAO-56 PM model.

## Methods

To develop and test the  $ET_o$  equations, weather data sets were retrieved from 106 locations that represent a range of climates across the contiguous United States (see Appendix I for data sources). These data were checked for integrity and quality. Then the PT and MK-Ha daily  $ET_o$  estimates were compared using the original coefficients at the 106 study sites with the FAO-56  $ET_o$  for the growing season period. This period may vary between the study sites as a function of climate, but for consistency the period of April 1 to September 30 was used for all stations and this time range is subsequently referred to as the growing season period.

In the second step for each station, the PT and MK-Ha evaporative coefficients,  $\alpha$  and  $C$ , were calibrated by minimizing the sum of the squared residuals between the benchmark FAO-56 PM  $ET_o$  and the PT and MK-Ha models. The calibrated PT and MK-Ha model predictions were then reevaluated. Next multiple linear regression techniques and the results from the previous step were

applied to develop coefficient adjustment relationships for the PT and MK-Ha models based on annual averages of RH and  $U$ . Once the equations were established, spatial distributions of annual RH (New et al. 2000) and  $U$  [National Renewable Energy Laboratory (NREL) 1986] were used to generate PT and MK-Ha coefficient maps for the contiguous United States. In the fourth step, the performance of the conditional coefficients were tested with weather data from 22 stations not included in the original data set. For these test stations, both coefficient values estimated with the annual RH and  $U$  from the station records and the map values calculated in the third step were used.

The effectiveness of the adjusted coefficients was evaluated using the root-mean square error (RMSE), the index of agreement  $d$  (Willmott 1982), and the ratio between the PT and MK-Ha  $ET_o$  and FAO-56 PM  $ET_o$ , for the growing season  $r$ . Equations used for these measures are

$$RMSE = \left[ N^{-1} \sum_i^N (ET_{o,pi} - ET_{o,i})^2 \right]^{0.5} \quad (4)$$

$$d = 1 - \left[ \frac{\sum_{i=1}^N (ET_{o,pi} - ET_{o,i})^2}{\sum_{i=1}^N (|ET'_{o,pi}| - |ET'_{o,i}|)^2} \right], \quad 0 \leq d \leq 1 \quad (5)$$

with  $ET'_{o,pi} = ET_{o,pi} - \overline{ET_o}$ ;  $ET'_{o,i} = ET_{o,i} - \overline{ET_o}$ ; and

$$r = \frac{\sum_i^N ET_{o,pi}}{\sum_i^N ET_{o,i}} \quad (6)$$

where  $i$  = index for the day;  $ET_{o,pi}$  = daily  $ET_o$  rates from either PT or MK-Ha; and  $ET_{o,i}$  = FAO-56 PM daily  $ET_o$  rate. The PT and MK-Ha methods approximate best the FAO-56 PM when the RMSE is small and when  $d$  and  $r$  approach unity.

## Meteorological Data Sets

The meteorological data sets were retrieved primarily from agricultural weather network sites that recorded hourly values of  $T$ ,  $R_s$ , RH, and  $U$ . Selected stations are from 106 locations shown in Fig. 1 as open circles, where circle size represents the estimated United Nations Environment Programme (UNEP) (1992) aridity index class  $AI_u$ , defined as the ratio between the annual precipitation and annual potential evapotranspiration. Larger circles are shown for humid climates, smaller circles for dry climates. Twenty-two additional stations in Fig. 1, shown as solid triangles, were used as test sites. The map was produced from USGS (2003) GIS data sets.

The criteria for selecting the locations shown in Fig. 1 were (1) availability of continuous and consistent hourly meteorological data ( $T$ , RH,  $U$ , and  $R_s$ ) for 3 to 5 years; and (2) representativeness for a range of climates and latitudes. The weather data time series from all stations were checked for continuity and quality. Linear interpolation was used for records with missing periods of less than 3 h. For longer periods, the filling guidelines provided in Allen et al. (1998) were used. Less than 5% of the data required any fill-in procedures. For 100 of the 106 stations, 5 years of data were used from each station, while for the remaining six stations, 4 years (five locations) and 3 years (one location) were considered. Daily average values of input weather variables were derived from the hourly data series.

Based on the Köppen-Geiger classification, the climate conditions vary significantly between the 106 sites (open circles) shown



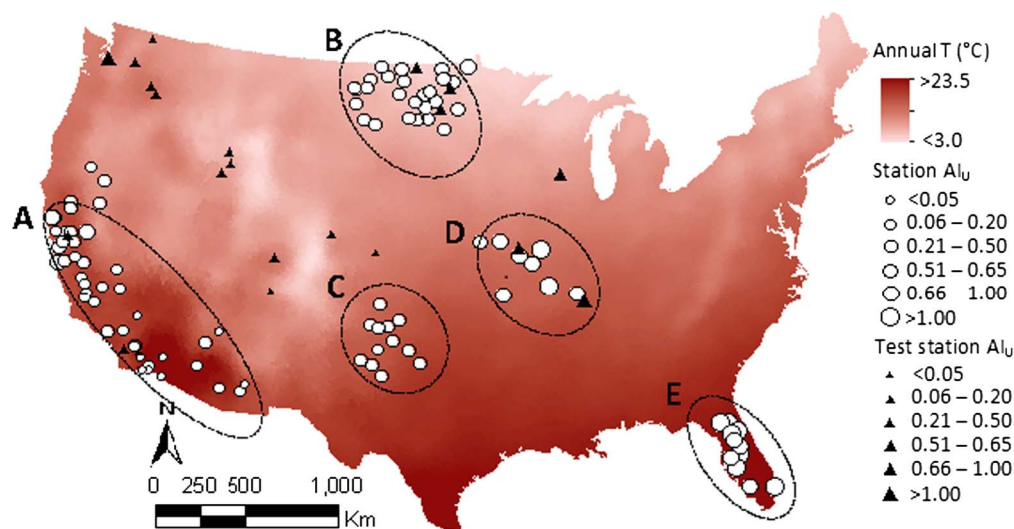


Fig. 1. Locations and UNEP aridity index of study and test sites displayed on the annual average air temperature U.S. map

in Fig. 1. In Region A, California and Arizona, they range from Mediterranean in the southern part to more continental inland, and to semiarid and arid in the southeastern areas. Most arid stations are located in Arizona, where annual averages of RH are low and mean annual  $T$  can reach 20–21°C. Region B has a continental climate, with the eastern part characterized by humid continental conditions with warm summers and cold winters and the western part by drier conditions with less precipitation. Generally, Region B has relatively low mean annual  $T$ , 3.8–7.2°C, and high mean annual  $U$ , 3.2–5.4  $\text{m} \cdot \text{s}^{-1}$ . The stations in Region C are mostly located in the Texas High Plains area characterized by a semiarid climate, with hot summers and significant temperature changes from day to night and mild winters. Stations in Region D have a humid continental climate with approximately 12–14°C mean annual  $T$ , with cold winters and hot summers and, at times, significant swings in air temperatures during the summer months. The climate of Region E (Florida) is humid subtropical in the north and tropical in the south, with long, humid, warm summers and mild winters with positive temperatures. Region E generally has high mean annual  $T$ , 20–24°C, high mean annual RH, 74–79%, and low mean  $U$ , typically less than 2  $\text{m} \cdot \text{s}^{-1}$ .

Regions A–E span a range of different climate types across the contiguous United States, as shown in the updated Köppen-Geiger map of Peel et al. (2007). (See Appendix I for details for accessing the Köppen-Geiger maps). Of the 22 test stations, shown as solid triangles in Fig. 1, eight were selected from regions A, B, and D and 14 from locations outside regions A–E. These additional locations include the mountainous areas in Idaho, maritime and humid western Washington, semiarid eastern Washington and Colorado, and continental Wisconsin. The annual average  $T$  at the test stations ranges from 4.8 to 22.7°C; the annual average RH and annual average  $U$  range from 46.7 to 79.1%, and 1.1 to 4.4  $\text{m} \cdot \text{s}^{-1}$ , respectively. Site characteristics are summarized in Appendix II.

## Results

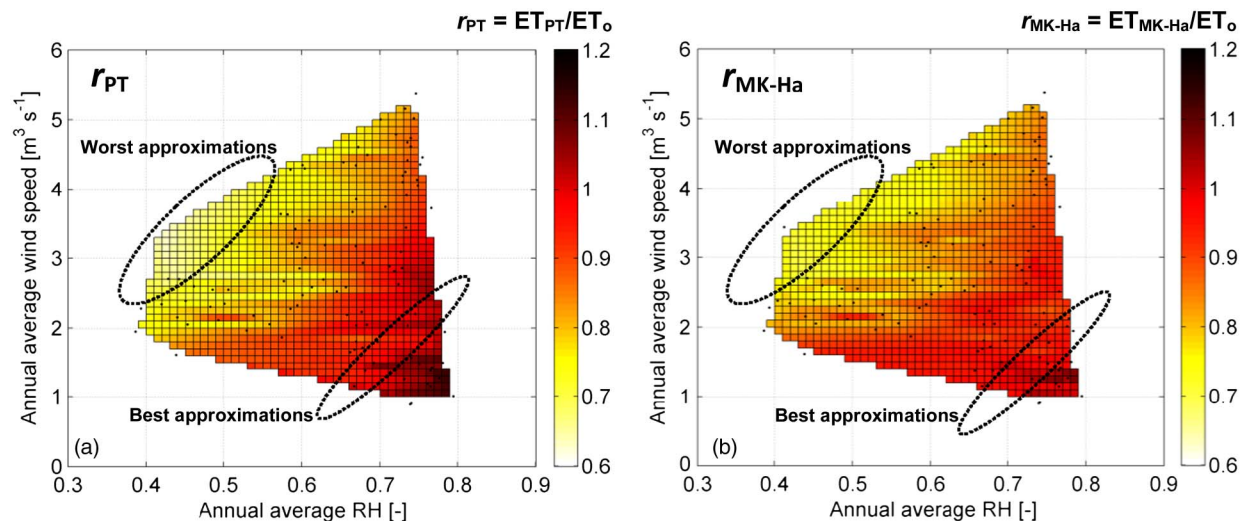
### Daily $ET_o$ Estimates Before and After Local Calibration

To compare PT and MK-Ha models to the FAO-56 PM equation, the ratios between the total growing season  $ET_o$  from the simpler models to the FAO-56 PM  $ET_o$ , referred to as  $r_{PT}$  and  $r_{MK-Ha}$  were

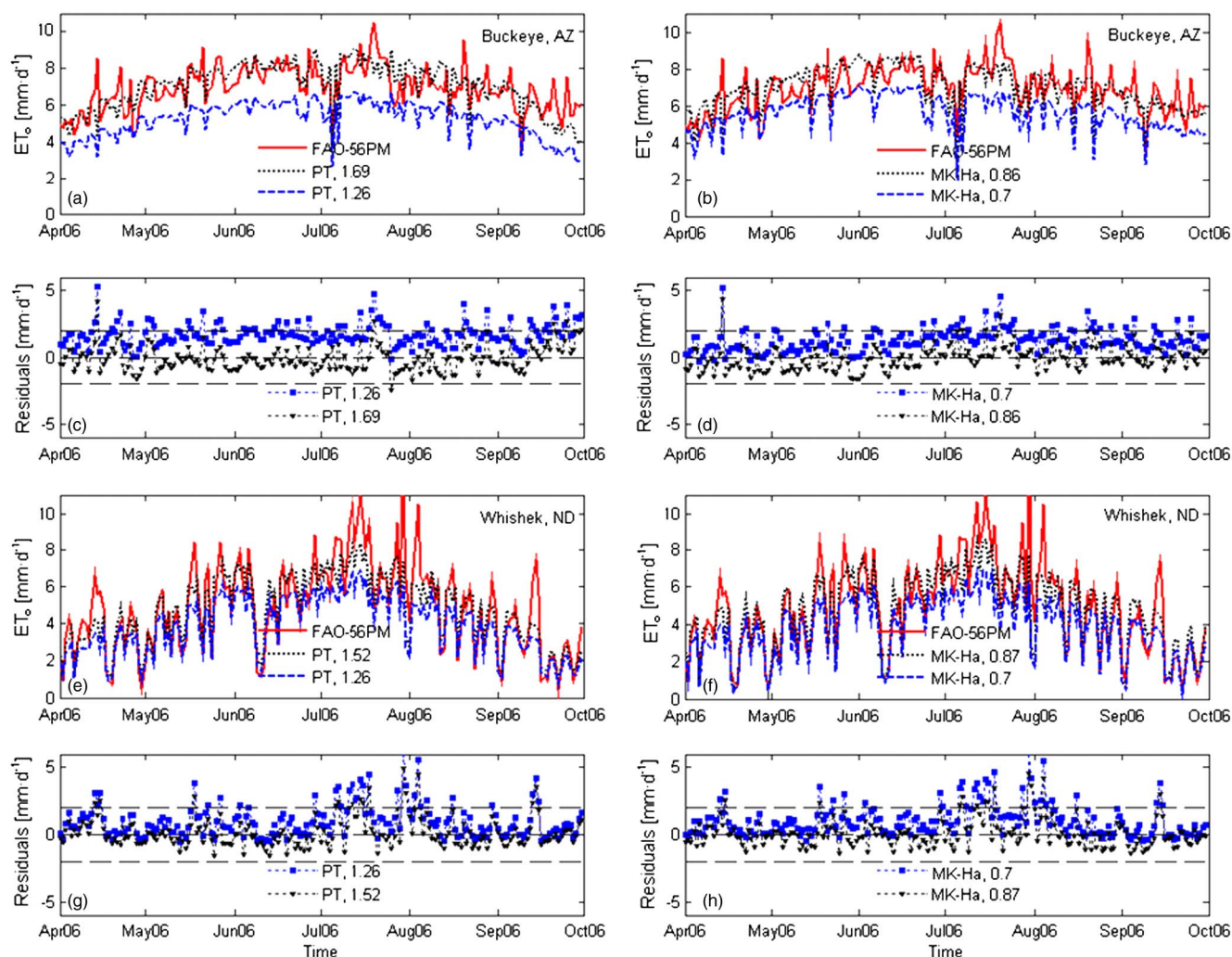
calculated. At humid and lower wind speed sites, the two methods estimated relatively well the FAO-56 PM  $ET_o$ . Fig. 2(a) shows that the PT model was within approximately 5% of the FAO-56 PM  $ET_o$  at sites where the annual RH ranged between 68 and 75% and annual  $U$  was less than approximately 2  $\text{m} \cdot \text{s}^{-1}$ . For annual RH larger than 75% and annual  $U$  less than 1.5  $\text{m} \cdot \text{s}^{-1}$ , the daily PT model overestimated the FAO-56 PM  $ET_o$ . Fig. 2(b) shows that the MK-Ha  $ET_o$  approximated best the FAO-56 PM  $ET_o$  at sites where the annual RH was generally higher than 70% and annual  $U$  was lower than 2  $\text{m} \cdot \text{s}^{-1}$ .

Fig. 3 shows examples of local calibration of the PT and MK-Ha daily  $ET_o$  models at two different stations: Buckeye, Arizona, and Wishek, North Dakota. The first station is located in an arid region characterized by high annual average  $T$  (21–22°C), low annual average RH (38–40%), high annual average  $R_s$  (235  $\text{W} \cdot \text{m}^{-2}$ ), and moderate annual average  $U$  (2  $\text{m} \cdot \text{s}^{-1}$ ). In contrast, the second station has low annual average  $T$  (5–6°C), high RH (73–75%), low  $R_s$  (160  $\text{W} \cdot \text{m}^{-2}$ ), and high  $U$  (5.6  $\text{m} \cdot \text{s}^{-1}$ ). Figs. 3(a and b) show that for the Arizona station at low RH conditions and relatively low  $U$ , the discrepancies between the simpler models and the FAO-56 PM  $ET_o$  were reduced through calibrating the evaporative coefficients, with the resulting residuals having a more uniform spread around zero. For the windy North Dakota site, the calibrated coefficients,  $\alpha$  and  $C$ , corrected the general trend of the PT and MK-Ha  $ET_o$  daily variations, but the highest FAO-56 PM  $ET_o$  rates remained underpredicted by the simpler models, even with the calibrated coefficients [Figs. 3(c and d)]. Plots are shown for the 2006 growing season.

The variability of the estimated  $r_{PT}$  and  $r_{MK-Ha}$  at all stations is also shown in Fig. 4(a) as box-and-whisker plots before calibration ( $r_{PT}$  and  $r_{MK-Ha}$ ) and after local calibration ( $r_{PT-c}$  and  $r_{MK-Ha-c}$ ). Outliers are defined to be outside of the  $Q_1 - 1.5 \cdot (Q_3 - Q_1)$  to  $Q_3 + 1.5 \cdot (Q_3 - Q_1)$  interval, where  $Q_1$  is the 25th percentile and  $Q_3$  is the 75th percentile in each of the four data sets. The values of  $r_{PT}$  and  $r_{MK-Ha}$  range over intervals from 0.62 to 1.14 and 0.70 to 1.10, respectively, with the lowest values at arid and windy sites and the highest values for the humid sites, as illustrated also in Fig. 2. Median values are 0.86 for both methods. Both  $r_{PT}$  and  $r_{MK-Ha}$  intervals were substantially reduced after calibration to 0.97 to 1.01, and 0.96 to 1.01, respectively [Fig. 4(a), last two box plots], with a median of 0.99 in both cases. The values of the calibrated PT  $\alpha_c$  and MK-Ha  $C_c$  coefficients ranged between 1.11 to 2.00 and



**Fig. 2.** (a) Ratios  $r_{PT}$  of the growing season PT  $ET_o$  to FAO-56 PM  $ET_o$ ; (b) MK-Ha  $ET_o$  to FAO-56 PM  $ET_o$  as a function of annual RH and  $U$ ; dots represent station-based calculations of  $r_{PT}$  and  $r_{MK-Ha}$ , and filled areas are developed from a projected triangle-based linear interpolation grid



**Fig. 3.** Examples of local calibration of the PT and MK-Ha models for April to October 2006 daily evaporation at (a)–(d) Buckeye, Arizona; (e)–(h) Whishek, North Dakota



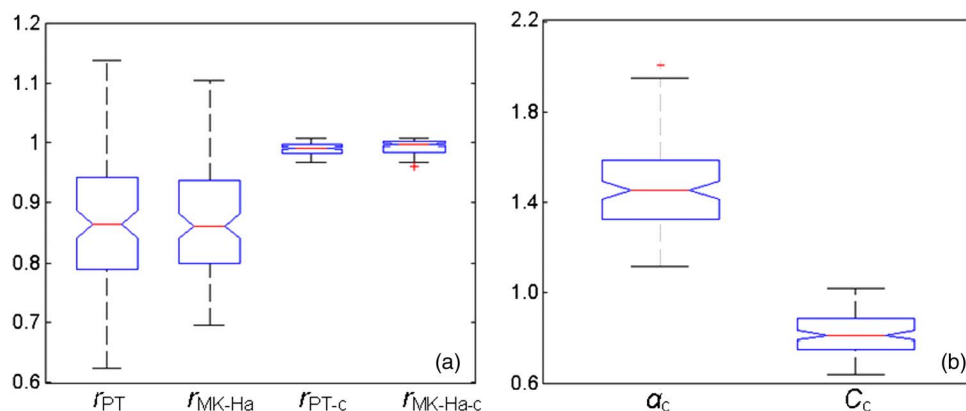


**Fig. 4.** (a) Ratios of the growing season PT ET<sub>o</sub> to FAO-56 PM ET<sub>o</sub> and MK-Ha ET<sub>o</sub> to FAO-56 PM ET<sub>o</sub> before and after local calibration; (b) ranges of the calibrated  $\alpha$  and  $C$

0.63 to 1.01, with higher values at low RH and windy sites and lower values at humid sites [Fig. 4(b)].

### Daily Evaporative Coefficients Relationships

Figs. 3 and 4(a) show that the site-calibrated evaporative coefficients improved the performance of the PT and MK-Ha ET<sub>o</sub> models, especially at dry and windy sites. To develop prediction equations for local  $\alpha$  and  $C$ , multiple linear regressions with mean annual RH (or mean annual VPD) and mean annual  $U$  as independent variables were used. The equations have the following generic form, for which coefficients  $b_1$ ,  $b_2$  and  $b_3$  were determined:

$$\alpha, C = b_1 + b_2 \cdot \text{RH (or VPD)} + b_3 \cdot U \quad (7)$$

where RH varies between 0 and 1, VPD is in kilopascals, and  $U$  is in meters per second (Fig. 5). Table 2 lists the  $b_{1,2,3}$  coefficients, the 95% confidence intervals (CIs) for each  $b$ , and the explained variance,  $r^2$ .

The variables, RH, and  $U$  (or VPD and  $U$ ) used in Eq. (7) were tested for linear dependence ( $r^2 = 0.01$  and  $0.14$ , respectively) and can be treated as independent. Coefficients  $\alpha$  and  $C$  had the strongest correlation (as a second-order polynomial) with annual RH (VPD), with the PT  $\alpha$  having the highest correlation ( $r^2 = 0.65$  with RH and  $r^2 = 0.40$  with VPD). The correlation was weaker with  $U$  and  $R_s$  and zero with annual  $T$ . The calibrated values of  $\alpha$  and  $C$  followed a linear relationship (Fig. 6).

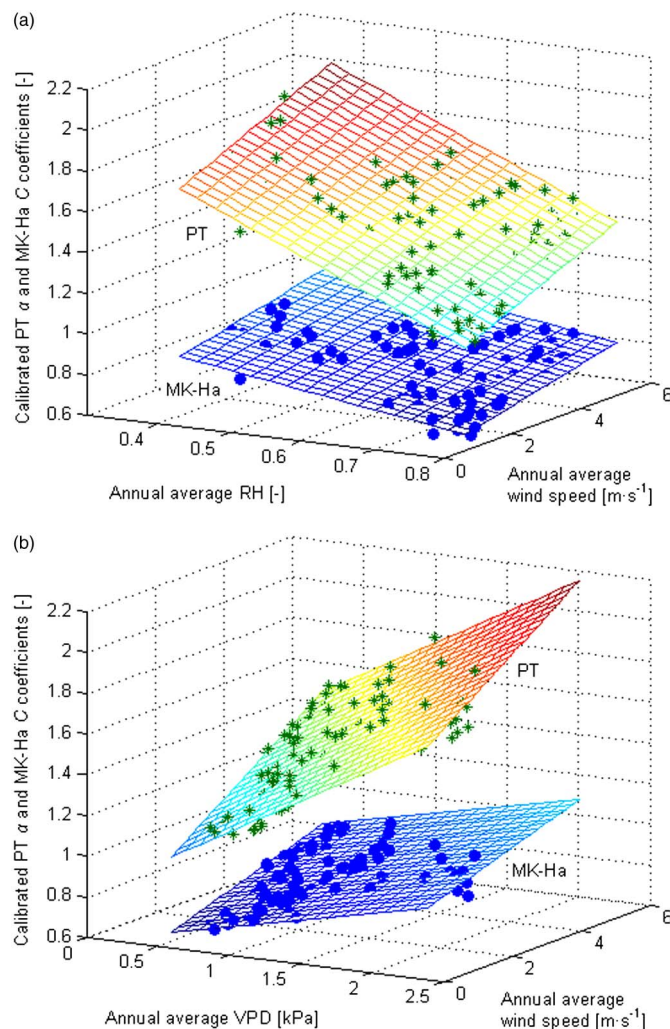
### Maps of Evaporative Model Coefficients

Maps of the PT and MK evaporative coefficients were generated for the contiguous United States based on Eq. (7) and the spatial distributions of annual average RH [New et al. (2000), Fig. 7(a)] and  $U$  derived from the NREL 1986 data set (see Appendix I for online resources). The NREL data set provides wind speed at 10-m height,  $U_{10}$ , shown in Fig. 7(b). This was further converted into  $U$  at 2-m height using the following correction formula (Allen et al. 1994):

$$U = U_z \left[ \frac{4.87}{\ln(67.8 \cdot z - 5.42)} \right] \quad (8)$$

where  $U_z = U_{10}$ ; and  $z = 10$  m. The maps in Figs. 7(c–d) show that larger values of  $\alpha$  and  $C$  were estimated for windy locations (e.g., mountainous areas) and low annual average RH areas (e.g., Arizona and eastern California), while smaller values were

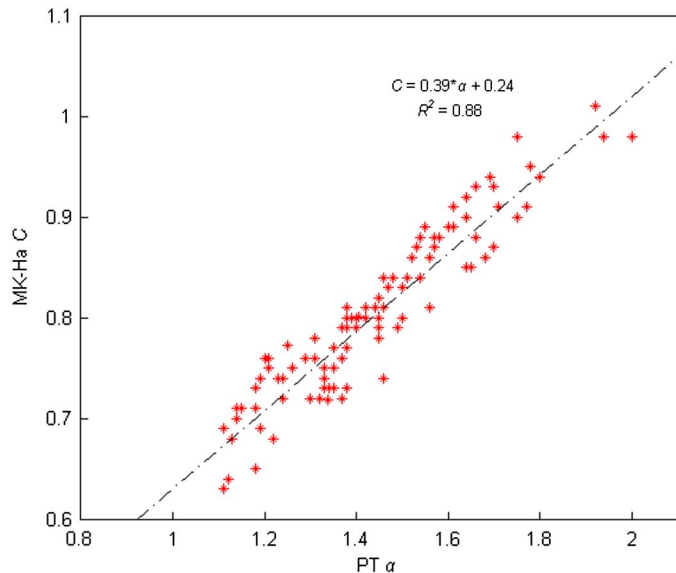
estimated for the humid and less windy areas such as the warm and humid southeastern region of the United States [Figs. 7(c–d)]. Details for obtaining ArcGIS coefficient maps are given in Appendix I.



**Fig. 5.** (a) Multiple linear regressions based on mean annual RH and  $U$ ; (b) VPD and  $U$  for the PT and MK-Ha ET<sub>o</sub> models' evaporative coefficients,  $\alpha$  and  $C$

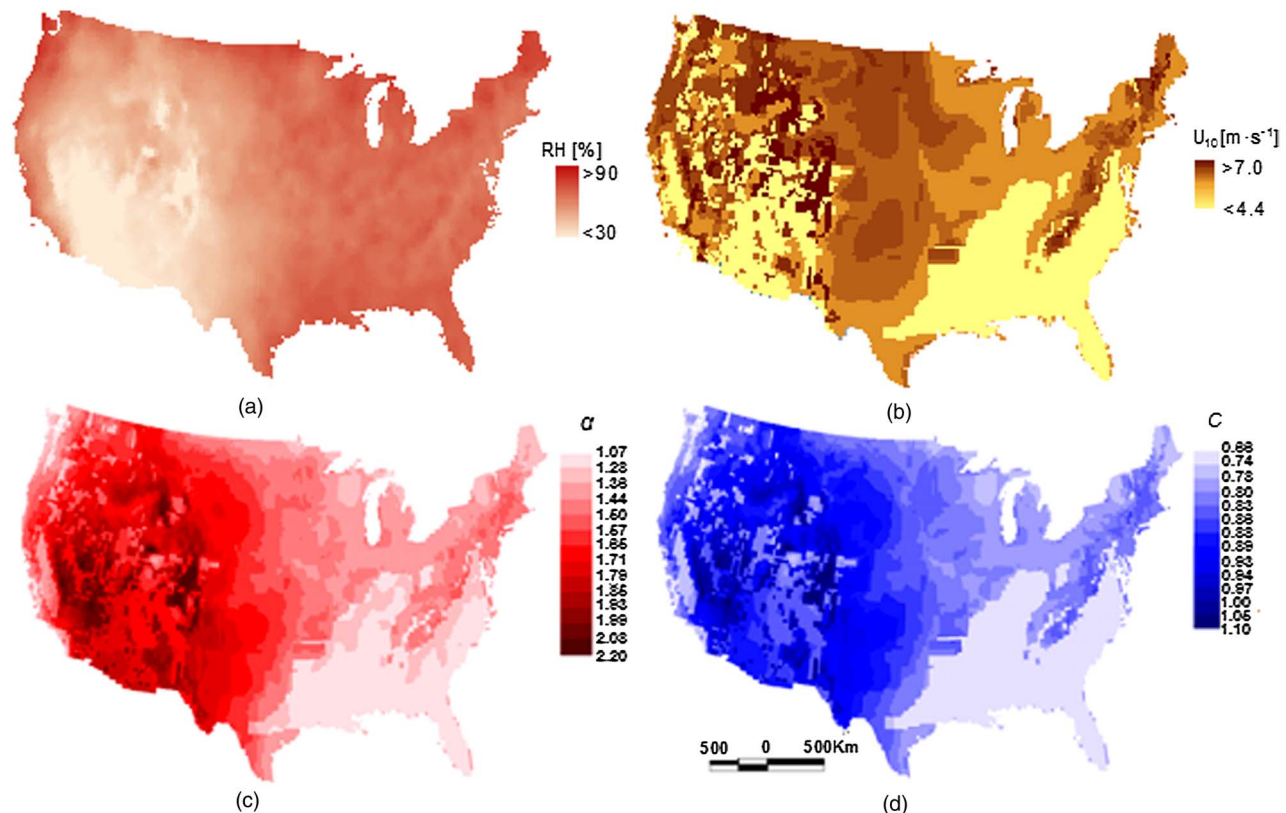
**Table 2.** Multiple Linear Regression Coefficients  $b_{1,2,3}$ , 95% CI and  $r^2$ 

Coefficient	$b_1$	95% CI $b_1$	$b_2$	95% CI $b_2$	$b_3$	95% CI $b_3$	$r^2$
$(\alpha)_{RH,U}$	2.214	2.116–2.311	–1.526	–1.668 to 1.384	0.079	0.065–0.092	0.84
$(C)_{RH,U}$	1.036	0.984–1.089	–0.527	–0.604 to –0.450	0.041	0.033–0.048	0.72
$(\alpha)_{VPD,U}$	0.717	0.647–0.786	0.387	0.349 to 0.426	0.122	0.107–0.138	0.85
$(C)_{VPD,U}$	0.493	0.467–0.519	0.152	0.137 to 0.166	0.058	0.052–0.064	0.82

**Fig. 6.** Linear relationship between the calibrated PT  $\alpha$  and MK-Ha  $C$  coefficients

### Model Tests

The PT and MK-Ha evaporative coefficients  $\alpha$  and  $C$  at the test stations were estimated in two ways: (1) using the annual average RH (or VPD) and  $U$  data from the station records in Eq. (7), and (2) extracting the coefficients from the generated coefficient maps showed in Figs. 7(c–d). The two sets of  $\alpha$  and  $C$  estimates are listed in Appendix II, which shows that generally there was good agreement between the station and map estimates of  $\alpha$  and  $C$ . All performance measures [Eqs. (4)–(6)] showed improvements in the PT and MK-Ha  $ET_o$  predictions when using either the station or the map coefficients compared with the original coefficient values. All models with revised coefficients show reduced ranges of RMSE,  $d$ , and  $r$  values relative to the values with the original coefficients (Fig. 8). The  $r$  performance statistic shows the greatest improvement, with median values increasing from  $<0.9$  for the original coefficients to within 5% of unity for all models with the revised coefficients [Fig. 8(c)]. Changes in RMSE and  $d$  were more variable between models. With the original coefficients, median RMSE values were close to 1 for both models and were reduced to 0.78–0.85 for the revised coefficients using either the RH and  $U$  equation or the map coefficients [Fig. 8(a)]. Median RMSE values did not change between the original coefficients

**Fig. 7.** (a) Spatial distributions of annual average RH; (b) annual average  $U_{10}$ ; (c)  $\alpha$ ; (d)  $C$  for the contiguous United States



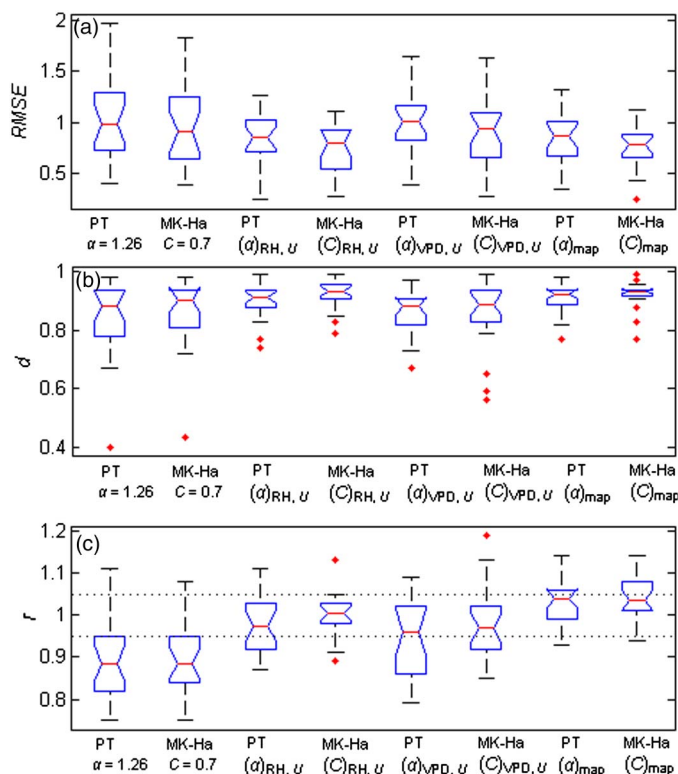


**Fig. 8.** Box plots of (a) RMSE; (b)  $d$ ; (c)  $r$  at the test stations for the original, station-specific, and map-derived  $\alpha$  and  $C$  coefficients; dotted lines in (c) identify the 0.95 and 1.05 values

and the coefficients from the VPD and  $U$  equation. Median values of  $d$  were approximately 0.9 for the original coefficients and did not significantly improve for the RH and  $U$  equation and the map coefficients, but the spread was greatly reduced [Fig. 8(b)]. Median values of  $d$  did not improve for the VPD and  $U$  equation.

The best-performing method based on the  $r$  criterion is the MK-Ha model with the coefficients adjusted based on the RH and  $U$  equation and station data, for which all values in the interquartile range fell within  $\pm 5\%$  of the FAO-56 PM  $ET_o$ . The map-derived coefficients improved the PT and MK-Ha model predictions and provided results comparable with those obtained by using the station coefficients.

In addition to numerical measures, scatterplots are useful to highlight discrepancies between the FAO-56 PM  $ET_o$  estimates and those of the simpler models (Willmott 1982). Scatterplots are shown for four example test stations (Puyallup, Washington; Spring Green, Wisconsin; Kettle Butte, Idaho; and Oasis, California), with site characteristics summarized in Appendix II. The PT and MK-Ha daily  $ET_o$  were plotted against the FAO-56 PM  $ET_o$  using the original coefficients [Figs. 9(a–d and i–l)] and the station-specific coefficients for both sets of independent variables RH and  $U$ , and VPD and  $U$ , respectively [Figs. 9(e–h and m–p)]. At the humid station (Puyallup, Washington), the PT and MK-Ha models approximated best the FAO-56 PM  $ET_o$ , at both low and high rates. As the annual average RH decreased and annual average  $U$  increased (Spring Green, Wisconsin, and Kettle Butte, Idaho), the scatter increased around the one-to-one line, especially at the more windy location (Kettle Butte, Idaho) where the highest FAO-56 PM  $ET_o$  rates remained underpredicted by both the PT and MK-Ha models. At the low RH station (Oasis, California), the adjusted coefficients corrected the general magnitude of the PT and MK-Ha

$ET_o$ , but considerable scatter around the one-to-one line remained. The RMSE,  $d$ , and  $r$  measures indicate that in general, performances of the PT and MK-Ha models with RH and  $U$  as independent variables for the evaporative coefficients  $\alpha$  and  $C$  were better than when using VPD and  $U$  as independent variables for a range of climates (Fig. 8). Among the sites shown in Fig. 9, the PT and MK-Ha models with the coefficients estimated using VPD and  $U$  approximated better FAO-56 PM at the Spring Green, Wisconsin, station only. The predicted PT and MK-Ha  $ET_o$  rates with RH and  $U$  as independent variables for the evaporative coefficient in Eq. (7) were slightly higher (less than 5%) than those estimated with VPD and  $U$  at all stations in Fig. 9, with the exception of the arid Oasis, California, location, where they were 5% lower.

## Discussion

The PT model with the original coefficient  $\alpha = 1.26$  underestimated the FAO-56 PM growing season  $ET_o$  at dry and windy sites. This behavior, also noted in studies that compared the PT  $ET_o$  estimates with lysimeter data [e.g., Berengena and Gavilán (2005) and Benli et al. (2010)], is expected because the original PT model was derived for low-wind conditions (Priestley and Taylor 1972). The largest discrepancies were found at arid and semiarid sites, where the estimated growing season  $ET_o$  was as low as 62 to 70% of the FAO-56 PM  $ET_o$  (Fig. 2). It was found that the original PT model approximated the growing season FAO-56 PM  $ET_o$  within approximately 5% at humid sites where the annual average RH ranged from 68 to 75% and  $U$  was less than  $2 \text{ m} \cdot \text{s}^{-1}$ .

At sites where annual average RH was higher than 75%, and annual average  $U$  was less than  $1.5 \text{ m} \cdot \text{s}^{-1}$ , the PT model overestimated the FAO-56 PM growing season  $ET_o$  [Fig. 2(a)]. For this data set,  $r_{PT}$  exceeded unity at 16 stations where annual RH varied between 68 and 79%. These stations were mostly located in Florida, Missouri, and coastal areas of California. Overestimations of the FAO-56 PM  $ET_o$  or lysimeter data by the original PT model were also reported for other humid sites. Suleiman and Hoogenboom (2007) found that the daily PT model overestimated the FAO-56 PM in the humid climate of Georgia, and Yoder et al. (2005) showed that the PT model overestimated lysimeter measurements in the humid climate of eastern Tennessee during the summer months when the monthly averages of RH and  $U$  varied between 76.4 and 83.5% and 0.9 and  $1.2 \text{ m} \cdot \text{s}^{-1}$ , respectively.

The MK-Ha model with the original coefficient  $C = 0.7$  compared well against lysimeter data at a humid site in Germany (Xu and Chen 2005), but the authors found no studies in which this model was applied for drier conditions and compared with the FAO-56 PM or measured data. At the study locations in this paper, the MK-Ha model with  $C = 0.7$  shows the same tendency as the PT model to underestimate the FAO-56 PM growing season  $ET_o$ , albeit to a slightly smaller degree [Fig. 2(b)]. The method approximated the FAO-56 PM best at sites where annual average RH was larger than 70% and  $U$  was less than  $2 \text{ m} \cdot \text{s}^{-1}$  [Fig. 2(b)].

Use of Eq. (7) to estimate the PT and MK-Ha coefficients improved the performance of the simpler models when compared with FAO-56 PM. Jensen et al. (1990) recommended a value of  $\alpha$  between 1.7 and 1.75 to improve the PT  $ET_o$  predictions at arid sites. The equations developed in this paper offer greater flexibility for a range of RH (or VPD) and  $U$  conditions. Spatial distributions (maps) of the PT and MK-Ha coefficients for the contiguous United States were also provided. Despite uncertainties associated with using the map coefficients [Figs. 7(c–d)], the PT and MK-Ha model predictions at 22 test stations improved over the original estimates and were of comparable accuracy with the corresponding

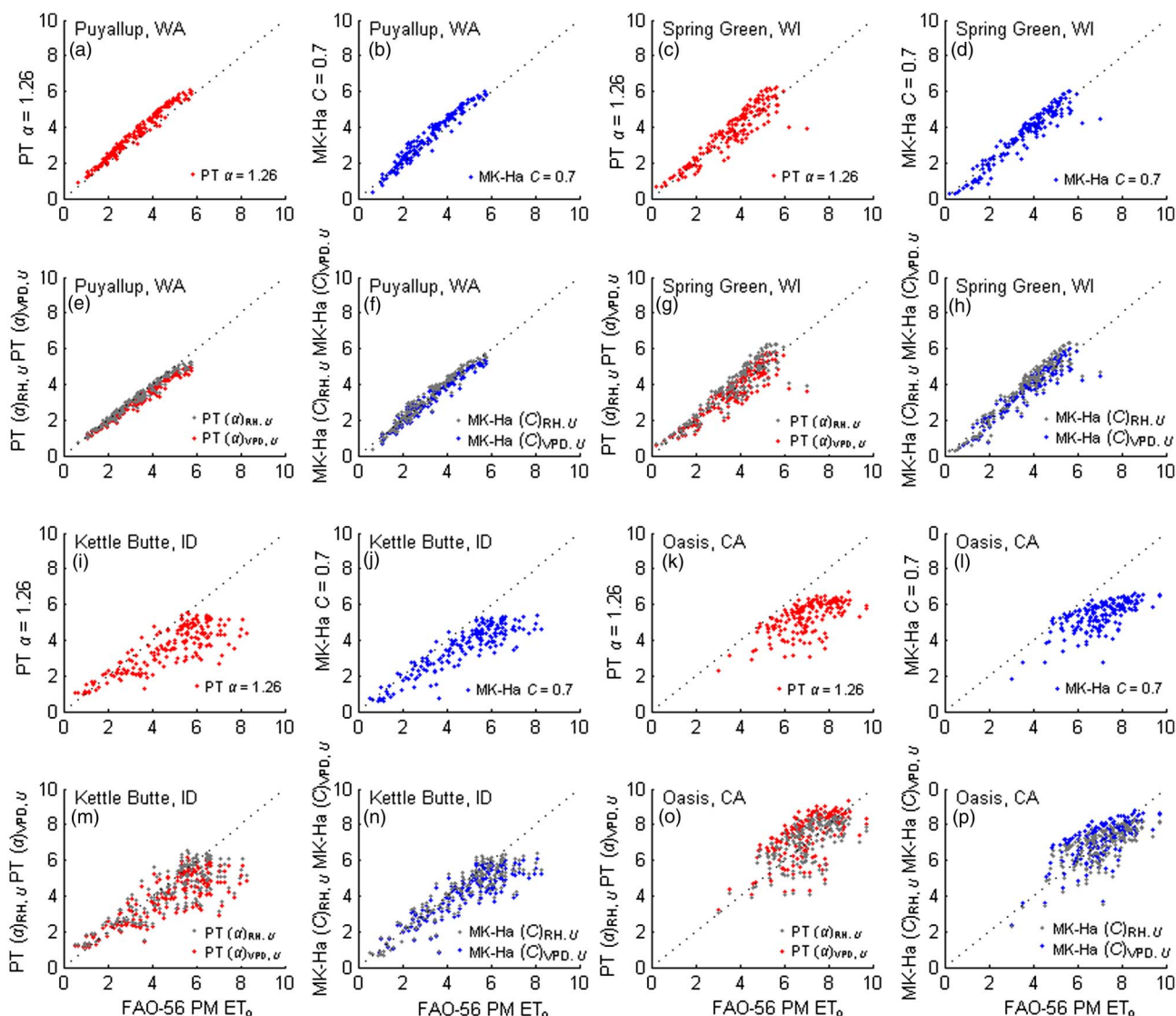


**Fig. 9.** Scatterplots of the FAO-56 PM  $ET_o$  and PT and MK-Ha  $ET_o$  in millimeters per day estimated (a)–(d) and (i)–(l) with the original coefficients; (e)–(h) and (m)–(p) with coefficients estimated based on the RH and  $U$  (light gray), and VPD and  $U$  (dark gray color) relationships, respectively, at four test stations; dotted line is the one-to-one relationship

predictions using the coefficients estimated from Eq. (7) and the station annual average RH and  $U$  data (Fig. 8). Uncertainties associated with the map coefficients are unquantifiable, but depend primarily on the quality of spatial data sets for RH and  $U$ , which in turn depend on the accuracy and robustness of point-measured data, uneven spatial coverage, and map interpolation techniques. The wind speed spatial data set includes additional uncertainty related to using the NREL data set to represent  $U_{10}$  and the conversion from  $U_{10}$  to  $U$  at 2-m height using Eq. (8).

Although the proposed relationships were developed using only weather station data from the contiguous United States, they covered a relatively large range of climate conditions represented by the annual average RH and  $U$  intervals shown in Fig. 2. Therefore, these relationships may be valid in other parts of the world within similar ranges. Extrapolation beyond these intervals will require additional testing.

The MK-Ha model is used much less frequently than the PT model, but the results in this paper show that compared with the PT model, the MK-Ha model offers three advantages. First it uses air temperature,  $T$ , and solar radiation,  $R_s$ , rather than the net

radiation,  $R_n$ , as input data. Net radiation  $R_n$  is not typically measured at standard weather stations, and its use in most  $R_n$ -based  $ET_o$  equations requires approximations and additional computational steps [e.g., Allen et al. (1998)]. Second, the MK-Ha model with the original  $C$  coefficient approximates the FAO-56 PM  $ET_o$  slightly better than the PT with the original coefficients [Figs. 2 and 3(a)]. Third, the variability of the calibrated  $C$  is smaller than the variability of calibrated  $\alpha$  [Fig. 3(b)], increasing the chance for better prediction of the FAO-56 PM  $ET_o$ .

The FAO-56 PM model was chosen as a base for comparison in place of observations due to the lack of measured reference evapotranspiration data over a wide enough range of climates. Similar approaches have been used [e.g., Irmak et al. (2003b)] based on the recommendation of the FAO Expert Consultation on Revision of FAO Methodologies for Crop Water Requirements (Smith et al. 1991) that empirical methods should be calibrated or validated for new regions using the FAO-56 PM equation. Limitations associated with data sets used include any undetected measurement errors in the weather variables and uncertainties associated with the annual average RH and  $U$  spatial distributions shown in Figs. 7(a–b).

## Summary and Conclusions

The performance of the PT and MK-Ha  $ET_o$  models with their original coefficients,  $\alpha = 1.26$  and  $C = 0.7$  respectively, were compared with the FAO-56 PM  $ET_o$  model using meteorological data from 106 stations that represent a relatively large range of climates across the contiguous United States. The original PT and MK-Ha models approximated best the FAO-56 PM  $ET_o$  at humid and less windy sites and underpredicted at drier sites and windier sites. The simpler models were closest to FAO-56 PM at sites where the annual mean RH was approximately 70% and annual 2-m wind speed ( $U$ ) was less than  $2 \text{ m} \cdot \text{s}^{-1}$ . Local calibration significantly improved the performance of the PT and MK-Ha models. At the study sites, locally calibrated PT and MK-Ha evaporative coefficients,  $\alpha_c$  and  $C_c$ , ranged between 1.11 and 2.00, and 0.63 and 1.01, respectively.

Equations were developed to estimate  $\alpha$  and  $C$  [Eq. (7)] for the PT and MK-Ha  $ET_o$  daily models using mean annual RH (or VPD) and 2-m elevation wind speed  $U$  as independent variables. The efficiency of these equations was tested at 22 stations not included in the original data set in two scenarios: (1) assuming that station annual average RH (or VPD) and  $U$  data are available, and (2) assuming that the RH and  $U$  data are not available, in which case site-specific model coefficients were taken from coefficient maps generated using existing spatial data sets of annual average RH and  $U$ . In both cases, the performance of the PT and MK-Ha models improved when compared with the estimates that used the original model coefficients. At the test sites, the improved models predicted  $ET_o$  values for the growing season within 5% of the FAO-56 PM  $ET_o$  values at 45–72% of stations and within 10% of FAO PM at 63–90% of stations. The best performing model was MK-Ha with coefficients estimated from annual average RH and  $U$ . The new PT and MK-Ha models can be used to improve  $ET_o$  estimates when spatial distributions of  $ET_o$  may be needed, such as in distributed hydrologic modeling or remote sensing applications.

The analysis in this paper shows that the MK-Ha model is preferable to the PT model because of its lower data requirements and smaller model coefficient variability over a range of climates. In cases in which only air temperature  $T$  is recorded at a station, the solar radiation  $R_s$  needed as input in the MK-Ha

model can be estimated with available  $R_s$  models [see, e.g., Allen et al. (1998)].

## Appendix I. Online Resources for Data Sets

Online resources for hourly weather data:

- Arizona Meteorological Network, AzMet (<http://ag.arizona.edu/AZMET/>);
- California Irrigation Management Information System, CIMIS (<http://www.cimis.water.ca.gov/cimis/welcome.jsp>);
- Colorado Agricultural Meteorological Network, CoAgMet (<http://ccc.atmos.colostate.edu/~coagmet/>);
- Florida Automated Weather Network (<http://fawn.ifas.ufl.edu/>);
- Missouri Historical Agricultural Weather Database (<http://agebb.missouri.edu/weather/history/>);
- North Dakota Agricultural Weather Network (<http://ndawn.ndsu.nodak.edu/>);
- Pacific Northwest Cooperative Agricultural Weather Network, AgriMet (<http://www.usbr.gov/pn/agrimet/>);
- Texas High Plains Evapotranspiration Network (<http://txhighplainset.tamu.edu/index.jsp>);
- Washington State University Weather Network (<http://weather.wsu.edu/>); and
- Wisconsin and Minnesota Cooperative Extension Agricultural Weather network (<http://www.soils.wisc.edu/wimnext/index.html>).

Online resources for the spatial data sets of relative humidity and wind data:

- Relative humidity data set: <http://www.sage.wisc.edu/atlas/maps.php?datasetid=53&includerelatedlinks=1&dataset=53>
- Wind power density class data set: <http://www.nrel.gov/gis/wind.html>

Updated Köppen-Geiger climate classification maps (Peel et al. 2007):

- <http://people.eng.unimelb.edu.au/mpeel/koppen.html>
- [http://people.eng.unimelb.edu.au/mpeel/Koppen/North\\_America.jpg](http://people.eng.unimelb.edu.au/mpeel/Koppen/North_America.jpg)

Priestley-Taylor and Makkink-Hansen revised coefficients for the continental United States: <https://catalyst.uw.edu/workspace/cristn/26054/166779> and <http://www.nrel.colostate.edu/kampf-research.html>.

## Appendix II. Test Stations

Test Stations and Their Latitude and Longitude, Annual Average Temperature ( $T$ ), RH, 2-m Wind Speed ( $U$ ), Solar Radiation ( $R_s$ ), and  $\alpha$  and  $C$  Values Estimated with Either Station Mean Annual RH and  $U$  or the Coefficient Maps in Figs. 7(c–d)

Station	Year	Latitude	Longitude	Elevation (m)	$T$ (°C)	RH (%)	$U$ ( $\text{m} \cdot \text{s}^{-1}$ )	$R_s$ ( $\text{W} \cdot \text{m}^{-2}$ )	$(\alpha)_{RH,U}^a$ (-)	$(C)_{RH,U}^b$ (-)	$(\alpha)_{VPD,U}^c$ (-)	$(C)_{VPD,U}^d$ (-)	$\alpha_{map}^e$ (-)	$C_{map}^f$ (-)
Aberdeen, Idaho	2002	42.9	112.8	1,341	6.5	64.7	2.9	164	1.45	0.81	1.35	0.77	1.6	0.87
Spring Green, Wisconsin	2003	43.2	89.9	220	7.9	73.4	2.2	159.6	1.27	0.74	1.18	0.70	1.39	0.80
Kettle Butte, Idaho	2006	43.5	112.3	1,565	6.8	63.9	3.2	154	1.49	0.83	1.40	0.79	1.60	0.87
Montevideo, Idaho	2005	44.0	112.5	1,480	5	69.4	2.0	153.8	1.31	0.75	1.20	0.70	1.65	0.89
Rolla, North Dakota	2006	48.8	99.6	552	4.8	74.4	3.9	157.2	1.39	0.8	1.37	0.79	1.36	0.80
Grand Forks, North Dakota	2002	47.8	97.1	257	5.3	75.4	3.5	145.7	1.34	0.78	1.31	0.76	1.40	0.81
Fingal, North Dakota	2002	46.8	97.8	438	5.2	76.5	4.4	149.7	1.39	0.81	1.42	0.82	1.42	0.82
Linneus, Missouri	2003	39.8	93.1	246	11.5	70.3	3.1	175.1	1.38	0.79	1.36	0.78	1.41	0.80
Oasis, California	2002	33.5	116.2	4	22.7	46.7	2.2	233.6	1.67	0.88	1.76	0.92	1.64	0.86
Charleston, Missouri	2004	36.9	89.3	98	14.5	74.8	2.7	173.2	1.29	0.75	1.28	0.74	1.28	0.74
Temecula East II, California	2003	33.5	117.0	468	16.1	65.1	1.8	212.6	1.36	0.77	1.37	0.77	1.39	0.77
Dixon, California	2004	38.4	121.8	37	14.5	74.0	3.3	207.7	1.34	0.78	1.45	0.82	1.50	0.84



## Appendix II. (Continued.)

Station	Year	Latitude	Longitude	Elevation (m)	$T$ (°C)	RH (%)	$U$ (m · s <sup>-1</sup> )	$R_s$ (W · m <sup>-2</sup> )	$(\alpha)_{RH,U}^a$ (-)	$(C)_{RH,U}^b$ (-)	$(\alpha)_{VPD,U}^c$ (-)	$(C)_{VPD,U}^d$ (-)	$\alpha_{map}^e$ (-)	$C_{map}^f$ (-)
Puyallup, Washington	2003	47.2	122.3	60	11.3	79.1	1.1	138.7	1.09	0.66	1.03	0.63	1.24	0.72
Wenatchee, Washington	2008	47.4	120.3	237	9.96	64.3	1.3	168.5	1.33	0.75	1.20	0.70	1.51	0.84
Grand Junction, Colorado	2005	39.2	108.6	1,484	11.3	50.9	1.9	194.8	1.59	0.85	1.41	0.78	1.60	0.85
Dove Creek, Colorado	2006	37.7	108.9	2,010	9.1	50.3	3.0	220.9	1.68	0.89	1.43	0.80	1.68	0.87
Wapato, Washington	2009	46.4	120.5	252	10.3	68.3	1.4	181.3	1.28	0.73	1.20	0.70	1.45	0.79
PK McClenny, Washington	2009	46.4	118.8	168	10.5	66.2	2.4	177.5	1.39	0.79	1.33	0.76	1.60	0.87
South Tonasket, Washington	2009	48.7	119.5	351	9.42	61.1	1.2	160.8	1.37	0.76	1.23	0.71	1.30	0.74
Walla Walla, Washington	2009	46.1	118.3	353	11.1	64.4	1.7	162.2	1.37	0.77	1.26	0.72	1.45	0.79
Idalia, Colorado	2006	39.7	102.1	1,212	10.8	60.73	3.5	191.3	1.561	0.86	1.51	0.84	1.66	0.90
Fort Collins, Colorado	2003	40.6	105.13	1,561	9.6	61.96	1.9	158.4	1.422	0.79	1.27	0.73	1.51	0.81

<sup>a</sup> $(\alpha)_{RH,U}$  is the PT coefficient predicted using Eq. (7) with station RH and  $U$  as independent variables.

<sup>b</sup> $(C)_{RH,U}$  is the MK-Ha coefficient predicted using Eq. (7) with station RH and  $U$  as independent variables.

<sup>c</sup> $(\alpha)_{VPD,U}$  is the PT coefficient predicted using Eq. (7) with station VPD and  $U$  as independent variables.

<sup>d</sup> $(C)_{VPD,U}$  is the MK-Ha coefficient predicted using Eq. (7) with station VPD and  $U$  as independent variables.

<sup>e</sup> $\alpha_{map}$  is the PT coefficient read at the site location from Fig. 7(c).

<sup>f</sup> $C_{map}$  is the MK-Ha coefficient read at the site location from Fig. 7(d).

## References

- Allen, R. G., Pereira, L. S., Raes, D., and Smith, M. (1998). "Crop evapotranspiration, guidelines for computing crop water requirements." *FAO Irrigation and Drainage Paper 56*, Food and Agriculture Organization of the United Nations, Rome.
- Allen, R. G., Smith, M., Perrier, A., and Pereira, L. S. (1994). "An update for the definition and calculation of reference evapotranspiration." *ICID Bull.*, 43(2), 1–34.
- Bandaragoda, C., Tarboton, D. G., and Woods, R. (2004). "Application of TOPNET in the distributed model intercomparison project." *J. Hydrol.*, 298(1–4), 178–201.
- Barton, I. J. (1979). "A parameterization of the evaporation from nonsaturated surfaces." *J. Appl. Meteorol.*, 18(1), 43–47.
- Bello, R. L., and Smith, J. D. (1990). "The effect of weather variability on the energy balance of a lake in the Hudson Bay Lowlands, Canada." *Arct. Alp. Res.*, 22(1), 98–107.
- Benli, B., Bruggeman, A., Oweis, T., and Ustun, H. (2010). "Performance of Penman-Monteith FAO56 in a semiarid highland environment." *J. Irrig. Drain. Eng.*, 136(11), 757–765.
- Berengena, J., and Gavilán, P. (2005). "Reference evapotranspiration estimation in a highly advective semiarid environment." *J. Irrig. Drain. Eng.*, 131(2), 147–163.
- Black, T. A. (1979). "Evapotranspiration from Douglas-fir stands exposed to soil water deficits." *Water Resour. Res.*, 15(1), 164–170.
- Bois, B., et al. (2008). "Using remotely sensed solar radiation data for reference evapotranspiration estimation at a daily time step." *Agric. For. Meteorol.*, 148(4), 619–630.
- Castellvi, F., Stockle, C. O., Perez, P. J., and Ibanez, M. (2001). "Comparison of methods for applying the Priestley-Taylor equation at a regional scale." *Hydrol. Processes*, 15(9), 1609–1620.
- Daneshkar Arasteh, P., and Tajrishy, M. (2008). "Calibrating Priestley-Taylor model to estimate open water evaporation under regional advection using volume balance method—Case study: Chahnimeh Reservoir, Iran." *J. Appl. Sci.*, 8(22), 4097–4104.
- Davies, J. A., and Allen, C. D. (1973). "Equilibrium, potential and actual evaporation from cropped surfaces in southern Ontario." *J. Appl. Meteorol.*, 12(4), 649–657.
- De Bruin, H. A. R. (1981). "The determination of (reference crop) evapotranspiration from routine weather data, in evaporation in relation to hydrology (technical meeting of the Committee for Hydrological Research, February, 1981)." *Comm. Hydrol. Res.*, 28, 25–37.
- De Bruin, H. A. R. (1987). "From Penman to Makkink." *Comm. Hydrol. Res.*, 39, 5–30.
- De Bruin, H. A. R., and Holtslag, A. A. M. (1982). "A simple parameterization of the surface fluxes of sensible and latent heat during daytime compared with the Penman-Monteith concept." *J. Appl. Meteorol.*, 21(11), 1610–1621.
- Eaton, A. K., Rouse, W. R., Lafleur, P. M., Marsh, P., and Blanken, P. D. (2001). "Surface energy balance of the western and central Canadian sub arctic: Variations in the energy balance among five major terrain types." *J. Clim.*, 14(17), 3692–3703.
- Fisher, J. B., DeBiase, T. A., Qi, Y., Xu, M., and Goldstein, A. H. (2005). "Evapotranspiration models compared on a Sierra Nevada forest ecosystem." *Environ. Model. Software*, 20(6), 783–796.
- Flint, A. L., and Childs, S. W. (1991). "Use of the Priestley-Taylor evaporation equation for soil water limited conditions in a small forest clear-cut." *Agric. For. Meteorol.*, 56(3–4), 247–260.
- Garcia, M., Raes, D., Allen, R., and Herbas, C. (2004). "Dynamics of reference evapotranspiration in the Bolivian highlands (Altiplano)." *Agric. For. Meteorol.*, 125(1–2), 67–82.
- Gavilán, P., Berengena, J., and Allen, R. G. (2007). "Measuring versus estimating net radiation and soil heat flux: Impact on Penman-Monteith reference ET estimates in semiarid regions." *Agric. Water Manage.*, 89(3), 275–286.
- Gavin, H., and Agnew, C. A. (2004). "Modelling actual, reference and equilibrium evaporation from a temperate wet grassland." *Hydrol. Processes*, 18(2), 229–246.
- Giles, D. G., Black, T. A., and Spittlehouse, D. L. (1985). "Determination of growing season soil water deficits on a forested slope using water balance analysis." *Can. J. For. Res.*, 15(1), 107–114.
- Hansen, S. (1984). "Estimation of potential and actual evapotranspiration." *Nordic Hydrol.*, 15(4–5), 205–212.
- Irmak, S., Allen, R. G., and Whitty, E. B. (2003a). "Daily grass and alfalfa-reference evapotranspiration estimates and alfalfa-to-grass evapotranspiration ratios in Florida." *J. Irrig. Drain. Eng.*, 129(5), 360–370.
- Irmak, S., Irmak, A., Allen, R. G., and Jones, J. W. (2003b). "Solar and net radiation-based equations to estimate reference evapotranspiration in humid climates." *J. Irrig. Drain. Eng.*, 129(5), 336–347.

- Jensen, M. E., Burman, R. D., and Allen, R. G., eds., (1990). *Evapotranspiration and irrigation water requirements*, ASCE Manuals and Reports on Engineering Practices No. 70, ASCE, New York.
- Jiang, L., and Islam, S. (2001). "Estimation of surface evaporation map over southern Great Plains using remote sensing data." *Water Resour. Res.*, 37(2), 329–340.
- Jury, W. A., and Tanner, C. B. (1975). "Advection modification of the Priestley and Taylor evapotranspiration formula." *Agron. J.*, 67(6), 840–842.
- Kustas, W. P., Stannard, D. I., and Allwine, K. J. (1996). "Variability in surface energy flux partitioning during Washita '92: Resulting effects on Penman-Monteith and Priestley-Taylor parameters." *Agric. For. Meteorol.*, 82(1–4), 171–193.
- López-Urrea, R., Martín de Santa Olalla, F., Fabeiro, C., and Moratalla, A. (2006). "An evaluation of two hourly reference evapotranspiration equations for semiarid conditions." *Agric. Water Manage.*, 86(3), 277–282.
- Makkink, G. F. (1957). "Testing the Penman formula by means of lysimeters." *J. Inst. of Water Eng.*, 11(3), 277–288.
- McNaughton, K. G., and Black, T. A. (1973). "A study of evapotranspiration from a Douglas Fir forest using the energy balance approach." *Water Resour. Res.*, 9(6), 1579–1590.
- Mukammal, E. I., and Neumann, H. H. (1977). "Application of the Priestley Taylor evaporation model to assess the influence of soil moisture on the evaporation from a large weighing lysimeter and class A pan." *Bound.-Lay. Meteorol.*, 12(2), 243–256.
- National Renewable Energy Laboratory (NREL). (1986). "Wind energy resource atlas of the United States." Golden, CO, ([http://redc.nrel.gov/wind/pubs/atlas/atlas\\_index.html](http://redc.nrel.gov/wind/pubs/atlas/atlas_index.html)) (Mar. 3, 2011).
- New, M. G., Hulme, M., and Jones, P. D. (2000). "Representing 20th century space-time climate variability. I: Development of a 1961–1990 mean monthly terrestrial climatology." 13(13), 829–856.
- Peel, M. C., Finlayson, B. L., and McMahon, T. A. (2007). "Updated world map of the Köppen-Geiger climate classification." *Hydrol. Earth Syst. Sci.*, 11(5), 1633–1644.
- Penman, H. L. (1948). "Natural evaporation from open water, bare soil, and grass." *Proc. R. Soc. London Ser. A*, 193(1032), 120–146.
- Pereira, A. R. (2004). "The Priestley-Taylor parameter and the decoupling factor for estimating reference evapotranspiration." *Agric. For. Meteorol.*, 125(3–4), 305–313.
- Price, J. S., Maloney, D. A., and Downey, F. G. (1991). "Peatlands of the Lake Melville coastal plain, Labrador." *Northern Hydrology Selected Perspectives: Proc., of the Northern Hydrology Symp.*, National Hydrology Research Institute, Saskatoon, SK, Canada, 293–302.
- Priestley, C. H. B., and Taylor, R. J. (1972). "On the assessment of surface heat flux and evaporation using large-scale parameters." *Mon. Weather Rev.*, 100(2), 81–92.
- Rouse, W. R., Mills, P. F., and Stewart, R. B. (1977). "Evaporation in high latitudes." *Water Resour. Res.*, 13(6), 909–914.
- Schramm, I., Boike, J., Bolton, W. R., and Hinzman, L. (2007). "Application of TopoFlow, a spatially distributed hydrologic model to the Imnavait Creek Watershed, Alaska." *J. Geophys. Res.*, 112(G4), G04S46.
- Shuttleworth, W. J., and Calder, I. R. (1979). "Has the Priestley-Taylor equation any relevance to forest evaporation?" *J. Appl. Meteorol.*, 18(5), 639–646.
- Smith, M., Allen, R. G., Monteith, J. L., Perrier, A., Pereira, L., and Segeren, A. (1991). "Report of the expert consultation on procedures for revision of FAO guidelines for prediction of crop water requirements." *Rep.*, Food and Agriculture Organization of the United Nations, Rome.
- Souch, C., Wolfe, C. P., and Grimmon, S. B. (1996). "Wetland evaporation and energy partitioning: Indian Dunes National Lakeshore." *J. Hydrol.*, 184(3–4), 189–208.
- Soylu, M. E., Istanbuluoglu, E., Lenters, J. D., and Wang, T. (2011). "Quantifying the impact of groundwater depth on evapotranspiration in a semi-arid grassland region." *Hydrol. Earth Syst. Sci.*, 15(3), 787–806.
- Stewart, R. B., and Rouse, W. R. (1976). "A simple method for determining the evaporation for shallow lakes and ponds." *Water Resour. Res.*, 12(4), 623–628.
- Suleiman, A. A., and Hoogenboom, G. (2007). "Comparison of Priestley-Taylor and FAO-56 Penman-Monteith for daily reference evapotranspiration estimation in Georgia." *J. Irrig. Drain. Eng.*, 133(2), 175–182.
- Tabari, H., and Hosseinzadeh Talaei, P. (2011). "Local calibration of the Hargreaves and Priestley-Taylor equations for estimating reference evapotranspiration in arid and cold climates of Iran based on the Penman-Monteith model." *J. Hydrol. Eng.*, 16(10), 837–847.
- United Nations Environment Programme (UNEP). (1992). *World atlas of desertification*, Edward Arnold, London.
- United States Geological Survey (USGS). (2003). "Hydrologic landscape regions of the United States." Reston, VA, (<http://water.usgs.gov/GIS/metadata/usgswrd/XML/hlrus.xml>) (Mar. 3, 2011).
- Wang, K., Li, Z., and Cribb, M. (2006a). "Estimation of evaporative fraction from a combination of day and night land surface temperatures and NDVI: A new method to determine the Priestley-Taylor parameter." *Remote Sens. Environ.*, 102(3–4), 293–305.
- Wang, X., Melesse, A. M., and Yang, W. (2006b). "Influences of potential evapotranspiration estimation methods on SWAT's hydrologic simulation in a northwestern Minnesota watershed." *Trans. ASABE*, 49(6), 1755–1771.
- Willmott, C. J. (1982). "Some comments on the evaluation of model performance." *Bull. Am. Meteorol. Soc.*, 63(11), 1309–1369.
- Xu, C.-Y., and Chen, D. (2005). "Comparison of seven models for estimation of evapotranspiration and groundwater recharge using lysimeter measurement data in Germany." *Hydrol. Processes*, 19(18), 3717–3734.
- Yoder, R. E., Odhiambo, L. O., and Wright, W. C. (2005). "Evaluation of methods for estimating daily reference crop evapotranspiration at a site in the humid Southeast United States." *Appl. Eng. Agric.*, 21(2), 197–202.
- Zhang, Y. Q., et al. (2004). "Energy fluxes and the Priestley-Taylor parameter over winter wheat and maize in the North China Plain." *Hydrol. Processes*, 18(12), 2235–2246.